HHS Public Access

Author manuscript

Oncogene. Author manuscript; available in PMC 2019 July 11.

Published in final edited form as:

Oncogene. 2019 April ; 38(17): 3316–3324. doi:10.1038/s41388-018-0668-3.

BTK SIGNALING DRIVES CD1d^{hi}CD5^{+} REGULATORY B CELL DIFFERENTIATION TO PROMOTE PANCREATIC CARCINOGENESIS

Shipra Das[1] and **Dafna Bar-Sagi**[1,*]

[1]Department of Biochemistry and Molecular Pharmacology, New York University School of Medicine, New York, NY 10016, USA

Abstract

The immune microenvironment of pancreatic ductal adenocarcinoma (PDAC) is comprised of a heterogeneous population of cells that are critical for disease evolution. Prominent among these are the specialized CD1d^{hi}CD5^{+} regulatory B (B_{reg}) cells that exert a pro-tumorigenic role by promoting tumor cell proliferation. Dissecting the molecular pathways regulating this immune sub-population can thus be valuable for uncovering potential therapeutic targets. Here, we investigate Bruton's Tyrosine Kinase (BTK), a key B cell kinase, as a potential regulator of CD1d^{hi}CD5^{+} B_{reg} differentiation in the pancreatic tumor microenvironment. Treatment of cytokine-induced B cells *in vitro* with the high specificity BTK inhibitor Tirabrutinib inhibited CD1d^{hi}CD5^{+} B_{reg} differentiation and production of IL-10 and IL-35, essential mediators of B_{reg} immunosuppressive functions. The BTK signaling pathway was also found to be active *in vivo* in PanIN-associated regulatory B cells. Tirabrutinib treatment of mice bearing orthotopic Kras^{G12D}-pancreatic lesions severely compromised stromal accumulation of the CD1d^{hi}CD5^{+} B_{reg} population. This was accompanied by an increase in stromal CD8^{+}IFNγ^{+} cytotoxic T cells and significant attenuation of tumor cell proliferation and PanIN growth. Our results uncover a novel role for BTK in regulating CD1d^{hi}CD5^{+} B_{reg} differentiation and emphasize its potential as a therapeutic target for pancreatic cancer.

Introduction

Pancreatic ductal adenocarcinoma (PDA), the most common type of pancreatic cancer, is one of the most aggressive solid malignancies (1). With a dismal 5-year survival rate of 5–7%, it is currently the third leading cause of cancer related mortality (2). In about 95% of cases, PDA initiates with the acquisition of an oncogenic mutation in *KRAS* and progresses through a distinct series of accumulating genetic and morphological alterations marked by

*Correspondence: dafna.bar-sagi@nyumc.org, Telephone: 212-263-2095, Address: 530 First Avenue, HCC 15, Executive Offices, New York, NY 10016.

Disclosure of Support

This work was funded in part by Gilead Sciences, Inc., Foster City, CA, USA.

Conflict of Interest

The authors declare that they have no conflict of interest.

tumor cell proliferation, apoptotic evasion, metabolic reprogramming and metastatic dissemination (3).

Additionally, PDA evolution is characterized by extensive stromal remodeling, with intense desmoplasia and robust immune cell infiltration (4, 5). The immune composition of the PDA microenvironment is sculpted early during transformation, culminating in the accumulation of immunosuppressive cell populations including regulatory T (T_{reg}) cells, myeloid-derived suppressor cells (MDSC), and tumor-associated macrophages (TAMs) (6, 7, 8). The tumor-protective role of these distinct cell populations in pancreatic neoplasia has been a subject of intense scrutiny. For instance, GM-CSF production by $KRas^{G12D}$-bearing pancreatic tumor cells promotes recruitment of MDSCs to the tumor microenvironment (TME), which in turn promote tumor growth by suppressing immune clearance by $CD8^+$ cytotoxic T (Tc) cells (7). Additionally, TAMs in the PDA microenvironment display a pro-tumorigenic M2-type polarization, which is characterized by expression of immunosuppressive molecules, including IL-10, Arginase 1, TGF-β, and CCl22 and promote a tolerant Th2 immune response (9). In keeping with the overall immune suppressive nature of the tumor microenvironment, the Th sub-types associated with pancreatic lesions are skewed towards the pro-tumorigenic Th2, T_{reg} and Th17 cells, relative to the Th1 population (6, 10, 11). Oncogenic Kras expression in cancer cells directly induces T_{reg} differentiation, which inhibits autoreactive Tc cells, thereby preventing immune clearance of the tumor (12, 13, 14). Furthermore, activation of $KRas^{G12D}$ expression specifically upon induction of pancreatitis, a major PDA risk factor, results in expansion of stromal $CD4^+T_{reg}$ and $CD4^+$ Th17 cell populations. Genetic depletion of $CD4^+$ T cells in this PDAC model resulted in de-repression of stromal $CD8^+$ Tc cells and subsequent attenuation of tumor progression (12).

Recently, tumor-infiltrating lymphocytic B (TIL-B) cells have been identified as significant positive regulators of PDA initiation and progression (15, 16, 17). Robust B cell infiltration is observed in the microenvironment of patient PDA samples. B cell depletion in early and advanced stage mouse models of pancreatic cancer was found to significantly attenuate tumor establishment and progression (17). Furthermore, in the *LSL-Kras^{G12D}; p48^{Cre}* (*KC*) mouse model of pancreatic intra-epithelial neoplasia (PanIN), we have previously uncovered a crucial role for a specialized B cell-subset in PanIN evolution (16). The PanIN microenvironment is enriched in IL-10 and IL-35 producing immunosuppressive $CD1d^{hi}CD5^+$ B regulatory (B_{reg}) cells, loss of which severely attenuates PanIN growth. We identified IL-35 as a prominent downstream effector of $CD1d^{hi}CD5^+$ B_{reg} function in pancreatic tumorigenesis by directly stimulating tumor cell proliferation (16). While the stromal-derived chemokine CXCL13 was found to potentiate B cell recruitment to the PanIN microenvironment (16), the molecular mechanisms regulating their further differentiation and function in the PanIN stroma remain unknown.

In light of these observations, we sought to dissect the molecular mechanisms regulating $CD1d^{hi}CD5^+$ B_{reg} expansion in the PanIN milieu. As a cytoplasmic non-receptor tyrosine kinase, the Bruton's Tyrosine Kinase (BTK) enzyme plays a central role in regulating B cell development and function, serving as a downstream signal transducer for a variety of cytokine and chemokine receptors, antigen receptors and integrins (18). BTK-mediated

signaling is in turn transmitted through several prominent downstream effectors including phosphoinositol-3 kinase (PI3K)-AKT, phospholipase-C (PLC), protein kinase C and nuclear factor κB (NF-κB) (19, 20). For instance, BTK activation upon antigen-mediated B cell receptor (BCR) engagement promotes B cell survival, proliferation and antibody production through PLCγ2 and subsequent NF-κB activation (21). Additionally, BTK is also a mediator of the TLR signaling pathway, wherein in complex with Myd88 it activates the NF-κB transcription factor and subsequently regulates expression of pro- and anti-inflammatory cytokines (22, 23).

While BTK-mediated regulation of the immunosupressive cytokine IL-10 has been described in macrophages and B cells (24, 25), its role in regulating B_{reg} biology remains unexplored. In the current study, we have uncovered a role for BTK as a critical regulator of $CD1d^{hi}CD5^{+}$ B_{reg} differentiation and immunosuppressive function. Furthermore, our findings point to a potential therapeutic strategy for targeting pancreatic cancer.

Results and discussion

We initiated our study by first investigating whether BTK activity is necessary for $CD1d^{hi}CD5^{+}$ B_{reg} evolution. To this end, we assessed the effect of the BTK inhibitor tirabrutinib on naïve murine splenic B cells treated with IL-6, IL-1β and α-CD40 antibody. These inflammatory signals, which are also enriched in the PanIN stroma (26), have been shown to induce differentiation of mouse splenic B_{reg} cells (27). Furthermore, both CD40 and the IL-6 receptor activate BTK (28, 29), as do the downstream effectors of the IL-1 receptor Myd88 and IRAK-1 (30), suggesting a role for BTK in B_{reg} differentiation induced by these pathways.

As illustrated in Fig 1a, b and Supplementary Figure S1a, inflammatory stimulation of splenic B cells from naïve mice upregulated BTK activation as measured by pBTK (Y223) expression (19). Cytokine treatment of B cells did not alter total BTK protein levels (Supplementary Fig. S1a). This increase was accompanied by an expansion of the $CD1d^{hi}CD5^{+}$ B_{reg} population (Fig. 1c, 1d). Significantly, inhibition of BTK activation by tirabrutinib (Fig. 1a, 1b, Supplementary Fig. S1a) attenuated cytokine-induced $CD1d^{hi}CD5^{+}$ B_{reg} differentiation (Fig. 1c, 1d). Furthermore, tirabrutinib markedly downregulated expression of both $CD1d^{hi}CD5^{+}$ B_{reg} functional markers, IL-10 (Fig. 1e, Supplementary Fig. S1b) and IL-35 (heterodimer of Ebi3 and p35, encoded by the *Ebi3* and *IL12A* genes, respectively) (Fig. 1f, 1g), which are critical mediators of $CD1d^{hi}CD5^{+}$ B_{reg} immunosuppressive function. Collectively, our results directly implicate the BTK signaling pathway in promoting $CD1d^{hi}CD5^{+}$ B_{reg} differentiation and production of the immunomodulatory cytokines IL-10 and IL-35.

To ascertain whether $CD1d^{hi}CD5^{+}$ B_{reg} evolution in pancreatic neoplasia is also regulated by BTK signaling, we first assessed the status of BTK activation in PanIN-associated B_{reg} cells. Immunostaining of tissue sections from LSL-$Kras^{G12D}$; p48-Cre (*KC)* (31) mice pancreata displayed co-localisation of pBTK (Y223) with IL-10 producing $CD19^{+}$ B cells (Fig. 2a, Supplementary Fig. S2a). We did not detect significant differences in overall BTK levels between regulatory and non-regulatory B cell populations in the *KC* pancreatic stroma

(Supplementary Fig. S2a). Furthermore, flow cytometric analysis of the pancreata of *KC* mice (Fig. 2b, Supplementary Fig. S2b) as well as orthotopically implanted $Kras^{G12D}$-PanIN lesions (7) (Supplementary Fig. S2c) revealed the expression of activated pBTK (Y223) specifically in PanIN-associated $CD1d^{hi}CD5^{+}$ B_{reg} cells. Plausible mechanisms for this observed BTK activation in stromal B cells include CD40, TLR4 and IL-6 signaling, all of which are enriched in the PanIN stroma (28, 29, 30, 32, 33, 34) and shown to regulate BTK activity. Interestingly, the TLR4 downstream effectors Myd88 and IRAK4 that mediate BTK phosphorylation are also interacting partners of the IL-1β receptor IL1R1. Since IL-1β is reported to be produced in pancreatic tumors (26), we sought to assess the contribution of IL-1β to BTK activation in PanIN-stromal B cells. Orthotopically implanted $Kras^{G12D}$-PanIN lesions were significantly enriched in IL-1β protein, relative to sham injections (Supplementary Fig. S2d). As outlined in Fig. 2c, $Kras^{G12D}$-PanIN lesions implanted in wild type or *IL1R1−/−* mouse pancreas were analysed for BTK (Y223) phosphorylation in PanIN-associated B cells. *IL1R1−/−* stromal B cells displayed significantly lower pBTK (Y223) levels relative to wild type control (Fig. 2d), indicating that IL-1 signaling in the PanIN TME contributes to BTK activation in stromal B cells.

We next sought to determine the functional significance of BTK activity in PanIN-associated $CD1d^{hi}CD5^{+}$ B_{reg} cells. Wild type mice bearing orthotopically implanted $Kras^{G12D}$-PanIN lesions were treated with tirabrutinib as outlined (Fig. 3a). Tirabrutinib inhibited BTK activation as measured by pBTK (Y223) staining in the PanIN stroma (Fig. 3b) and more specifically in infiltrating B cells (Fig. 3c, Supplementary Fig. S3a). Considering the crucial role of BTK in B cell proliferation and survival, we analyzed the effect of tirabrutinib treatment on both $CD1d^{hi}CD5^{+}$ B_{reg} cells and the overall tumor-infiltrating B cell population. BTK inhibition did not significantly alter the total $CD19^{+}$ B cell fraction in the tumor stroma after 2 weeks of tirabrutinib treatment (Fig. 3d; Supplementary Fig. S3b, S3c). On the other hand, the $CD1d^{hi}CD5^{+}$ B_{reg} subset displayed remarkable sensitivity to BTK inhibition, with a significant decrease in the stromal population within 2 weeks of treatment, relative to the vehicle control (Fig. 3e; Supplementary Fig. S3d, S3e). Prolonged tirabrutinib treatment for 4 weeks induced a small but significant decrease in stromal $CD19^{+}$ B cells (Fig. 3d; Supplementary Fig. S3b) while markedly decreasing the $CD1d^{hi}CD5^{+}$ B_{reg} population, relative to vehicle control (Fig. 3e; Supplementary Fig. S3d). $CD1d^{hi}CD5^{+}$ B_{reg} cells primarily mediate immunosupression by inhibiting Tc cell activation (35). Consistent with this, $CD1d^{hi}CD5^{+}$ B_{reg} depletion upon BTK inhibition was accompanied by a significant increase in the $IFN\gamma^{+}CD8^{+}$ Tc cell population (Fig. 3f; Supplementary Fig. S3f) without altering the overall $CD8^{+}$ Tc cell proportion (Supplementary Fig. S3g), further implicating BTK in the immunomodulatory function of $CD1d^{hi}CD5^{+}$ B_{reg}.

The physiologic importance of $CD1d^{hi}CD5^{+}$ B_{reg} attenuation upon BTK inhibition is highlighted by the reduced growth of the PanIN lesions (Fig. 4a and 4b). Tirabrutinib significantly inhibited proliferation of the tumor cells, relative to the vehicle control (Fig. 4c and 4d), as measured by immunohistochemical staining of the proliferation marker phospho-Histone H3 staining in the $Kras^{G12D}$-transformed epithelia. We did not detect induction of apoptosis upon tirabrutinib treatment, as assessed by cleaved caspase 3 staining (data not shown). This is consistent with our previously reported observation that the attenuation of PanIN growth in the absence of stromal $CD1d^{hi}CD5^{+}$ B_{reg} cells is due to inhibition of

epithelial proliferation (16). Taken together our observations implicate BTK in the development of pancreatic neoplasia through the regulation of $CD1d^{hi}CD5^{+}$ B_{reg} differentiation in the PanIN microenvironment.

Given the critical role of immunomodulation in promoting pancreatic tumorigenesis, understanding the molecular mechanisms mediating this process is essential for developing effective immunotherapeutic strategies for combating the disease. Initial efforts with checkpoint inhibitors such as α-CTLA-4 and α-PD-1 which show promise in other cancers have proved ineffective for pancreatic cancer (36), underscoring the need to identify and therapeutically explore additional targets.

In our pre-clinical model of pancreatic neoplasia, the observed decrease in stromal $CD1d^{hi}CD5^{+}$ B_{reg} population upon BTK inhibition is accompanied by significant attenuation of $Kras^{G12D}$-epithelial proliferation and PanIN growth. Additionally, BTK inhibition also led to a small but significant engagement of the Tc cell response, as measured by increased IFNγ production in $CD8^{+}$ T cells. Our results thus indicate that combining the cytostatic effect of BTK inhibitors with checkpoint-directed immunotherapy, which can further enhance the Tc cell response, may provide an effective multipronged approach for PDA therapy. BTK inhibitors are already approved as monotherapy for B cell malignancies (37), while clinical trials assessing the efficacy of BTK inhibitors in combination with anti-PD-1 immunotherapy are currently underway (e.g.-clinicaltrials.gov; NCT02362048).

In addition to pancreatic cancer, regulatory B cells have also been found to promote other tumor types including melanoma, mammary and squamous cell carcinoma (38). As such, understanding the molecular pathways regulating their development and function is of great importance. Unlike regulatory T cells, regulatory B lymphocytes are a heterogeneous population without well-defined precursors or developmental lineage (35). Instead, these cells exhibit great plasticity, differentiating in response to extracellular inflammatory cues from their microenvironment. While some of these inflammatory signals have been described, the downstream molecular pathways regulating the process remain to be elucidated. We have identified BTK as a direct cell-intrinsic regulator of $CD1d^{hi}CD5^{+}$ B_{reg} differentiation. BTK inhibition downregulates expression of the cytokines IL-10 and IL-35, expanding its potential role to additional immunosuppressive B cell subsets such as the i35-B_{reg} population as well as in various autoimmune conditions (39, 40). Further characterization of this pathway would not only enable a deeper understanding of this hitherto elusive B cell sub-population but also expand our repertoire of potential therapeutic candidates for immunotherapy.

Supplementary Material

Refer to Web version on PubMed Central for supplementary material.

Acknowledgement

The authors thank L.J. Taylor for help with article preparation and members of the Bar-Sagi lab for valuable discussions and comments. The authors also thank NYU Langone's Cytometry and Cell Sorting Laboratory, which is supported in part by grant P30CA016087 from the National Institutes of Health/ National Cancer Institute, for providing cell sorting/flow cytometry technologies. This work was supported in part by Gilead Sciences, Inc.,

Foster City, CA, USA, by NIH/NCI grant CA210263 (D. Bar-Sagi) and by The Lustgarten Foundation Pancreatic Cancer Convergence Dream Team grant SU2C-AACR-DT14-14 (to D.B.S.). Stand Up To Cancer is a program of the Entertainment Industry Foundation administered by the American Association for Cancer Research.

Competing Interests Statement: This work was supported in part by Gilead Sciences, Inc., Foster City, CA, USA, and by NIH/NCI grant CA210263 (D. Bar-Sagi). The authors declare that they have no conflict of interest.

References

1. Ryan DP, Hong TS, Bardeesy N Pancreatic adenocarcinoma. N Engl J Med 2014; 371:1039–49. [PubMed: 25207767]
2. Rahib L, Fleshman JM, Matrisian LM, Berlin JD 2016. Evaluation of pancreatic cancer clinical trials and benchmarks for clinically meaningful future trials: A systematic review. JAMA Oncol 2016; 2:1209–16. [PubMed: 27270617]
3. Rishi A, Goggins M, Wood LD, Hruban RH Pathological and molecular evaluation of pancreatic neoplasms. Semin Oncol 2015; 42:28–39. [PubMed: 25726050]
4. Stromnes IM, DelGiorno KE, Greenberg PD, Hingorani SR. Stromal reengineering to treat pancreas cancer. Carcinogenesis 2014; 35:1451–60. [PubMed: 24908682]
5. Vonderheide RH, Bayne LJ. Inflammatory networks and immune surveillance of pancreatic carcinoma. Curr Opin Immunol 2013; 25:200–5. [PubMed: 23422836]
6. Hiraoka N, Onozato K, Kosuge T, Hirohashi S Prevalence of FOXP3+ regulatory T cells increases during the progression of pancreatic ductal adenocarcinoma and its premalignant lesions. Clin Cancer Res 2006; 12:5423–34. [PubMed: 17000676]
7. Pylayeva-Gupta Y, Lee KE, Hajdu CH, Miller G, Bar-Sagi D Oncogenic Kras-induced GM-CSF production promotes the development of pancreatic neoplasia. Cancer Cell 2012; 21:836–47. [PubMed: 22698407]
8. Kurahara H, Shinchi H, Mataki Y, Maemura K, Noma H, Kubo F, et al. Significance of M2-polarized tumor-associated macrophage in pancreatic cancer. J Surg Res 2011; 167:e211–9. [PubMed: 19765725]
9. Mielgo A, Schmid MC Impact of tumour associated macrophages in pancreatic cancer. BMB Rep 2013 3; 46:131–8. [PubMed: 23527856]
10. McAllister F, Bailey JM, Alsina J, Nirschl CJ, Sharma R, Fan H, et al. Oncogenic Kras activates a hematopoietic-to-epithelial IL-17 signaling axis in preinvasive pancreatic neoplasia. Cancer Cell 2014; 25:621–37 [PubMed: 24823639]
11. De Monte L, Reni M, Tassi E, Clavenna D, Papa I Recalde H et al. Intratumor T helper type 2 cell infiltrate correlates with cancer-associated fibroblast thymic stromal lymphopoietin production and reduced survival in pancreatic cancer. J Exp Med 2011; 208:469–78. [PubMed: 21339327]
12. Zhang Y, Yan W, Mathew E, Bednar F, Wan S, Collins MA, et al. CD4+ T lymphocyte ablation prevents pancreatic carcinogenesis in mice. Cancer Immunol Res 2014; 2:423–35. [PubMed: 24795355]
13. Zdanov S, Mandapathil M, Abu Eid R, Adamson-Fadeyi S, Wilson W, Qian J, et al. Mutant KRAS Conversion of Conventional T Cells into Regulatory T Cells. Cancer Immunol Res 2016; 4:354–65. [PubMed: 26880715]
14. Granville CA, Memmott RM, Balogh A, Mariotti J, Kawabata S, Han W, et al. A central role for Foxp3+ regulatory T cells in K-Ras-driven lung tumorigenesis. PLoS One 2009; 4:e5061. [PubMed: 19330036]
15. Gunderson AJ, Kaneda MM, Tsujikawa T, Nguyen AV, Affara NI, Ruffell B, et al. Bruton Tyrosine Kinase-Dependent Immune Cell Cross-talk Drives Pancreas Cancer. Cancer Discov 2016; 6:270–85. [PubMed: 26715645]
16. Pylayeva-Gupta Y, Das S, Handler JS, Hajdu CH, Coffre M, Koralov SB, et al. IL35-Producing B Cells Promote the Development of Pancreatic Neoplasia. Cancer Discov 2016; 6:247–55. [PubMed: 26715643]
17. Lee KE, Spata M, Bayne LJ, Buza EL, Durham AC, Allman D, et al. Hif1a Deletion Reveals Pro-Neoplastic Function of B Cells in Pancreatic Neoplasia. Cancer Discov 2016; 6:256–69. [PubMed: 26715642]

18. Ponader S, Burger JA Bruton's tyrosine kinase: from X-linked gammaglobulinemia toward targeted therapy for B-cell malignancies. J Clin Oncol 2014 6 10; 32:1830–9. [PubMed: 24778403]
19. Mohamed AJ, Yu L, Backesjo CM, Vargas L, Faryal R, Aints A et al. Bruton's tyrosine kinase (Btk): function, regulation, and transformation with special emphasis on the PH domain. Immunol Rev 2009; 228:58–73. [PubMed: 19290921]
20. Petro JB, Khan WN. Phospholipase C-gamma 2 couples Bruton's tyrosine kinase to the NF-kappaB signaling pathway in B lymphocytes. J Biol Chem 2001; 276:1715–19. [PubMed: 11042193]
21. Burger JA, Wiestner AN. Targeting B cell receptor signaling in cancer: preclinical and clinical advances. Nat Rev Cancer 2018; 18:148–67. [PubMed: 29348577]
22. Isaza-Correa JM, Liang Z, van den Berg A, Diepstra A, Visser L. Toll-like receptors in the pathogenesis of human B cell malignancies. J Hematol Oncol 2014; 7:57. [PubMed: 25112836]
23. Doyle SL, Jefferies CA, Feighery C, O'Neill LA. Signaling by Toll-like receptors 8 and 9 requires Bruton's tyrosine kinase. J Biol Chem 2007; 282:36953–60. [PubMed: 17932028]
24. Schmidt NW, Thieu VT, Mann BA, Ahyi AN, Kaplan MH Bruton's tyrosine kinase is required for TLR-induced IL-10 production. J Immunol 2006; 177:7203–10. [PubMed: 17082638]
25. Corneth OB, de Bruijn MJ, Rip J, Asmawidjaja PS, Kil LP, Hendriks RW Enhanced Expression of Bruton's Tyrosine Kinase in B Cells Drives Systemic Autoimmunity by Disrupting T Cell Homeostasis. J Immunol 2016 ;197 :58–67. [PubMed: 27226091]
26. Delitto D, Black BS, Sorenson HL, Knowlton AE, Thomas RM, Sarosi GA et al. The inflammatory milieu within the pancreatic cancer microenvironment correlates with clinicopathologic parameters, chemoresistance and survival. BMC Cancer 2015; 15:783. [PubMed: 26498838]
27. Rosser EC, Oleinika K, Tonon S, Doyle R, Bosma A, Carter NAet al. Regulatory B cells are induced by gut microbiota-driven interleukin-1β and interleukin-6 production. Nat Med 2014; 20:1334–9. [PubMed: 25326801]
28. Brunner C, Avots A, Kreth HW, Serfling E, Schuster V Bruton's tyrosine kinase is activated upon CD40 stimulation in human B lymphocytes. Immunobiology 2002; 206:432–40. [PubMed: 12437073]
29. Matsuda T, Takahashi-Tezuka M, Fukada T, Okuyama Y, Fujitani Y, Tsukada S et al. Association and activation of Btk and Tec tyrosine kinases by gp130, a signal transducer of the interleukin-6 family of cytokines. Blood 1995; 85:627–33. [PubMed: 7530500]
30. Jefferies CA, Doyle S, Brunner C, Dunne A, Brint E, Wietek C et al. Bruton's tyrosine kinase is a Toll/interleukin-1 receptor domain-binding protein that participates in nuclear factor kappaB activation by Toll-like receptor 4. J Biol Chem 2003; 278:26258–64. [PubMed: 12724322]
31. Hingorani SR, Petricoin EF, Maitra A, et al. Preinvasive and invasive ductal pancreatic cancer and its early detection in the mouse. Cancer Cell 2003; 4: 437–50. [PubMed: 14706336]
32. Ochi A, Nguyen AH, Bedrosian AS, Mushlin HM, Zarbakhsh S, Barilla R, et al. MyD88 inhibition amplifies dendritic cell capacity to promote pancreatic carcinogenesis via Th2 cells. J Exp Med 2012; 209:1671–87. [PubMed: 22908323]
33. Unek T, Unek IT, Agalar AA, Sagol O, Ellidokuz H, Ertener O et al. CD40 expression in pancreatic cancer. Hepatogastroenterology 2013; 60:2085–93. [PubMed: 24719952]
34. Zhu Z, Aref AR, Cohoon TJ, Barbie TU, Imamura Y, Yang S, et al. Inhibition of KRAS-driven tumorigenicity by interruption of an autocrine cytokine circuit. Cancer Discov 2014; 4:452–65. [PubMed: 24444711]
35. DiLillo DJ, Matsushita T, Tedder TF B10 cells and regulatory B cells balance immune responses during inflammation, autoimmunity, and cancer. Ann N Y Acad Sci 2010; 1183:38–57. [PubMed: 20146707]
36. Zhang J, Wolfgang CL, Zheng L Precision Immuno-Oncology: Prospects of Individualized Immunotherapy for Pancreatic Cancer. Cancers (Basel) 2018; 10.pii:E39.
37. Tai YT, Chang BY, Kong SY, Fulciniti M, Yang G, Calle Y, Hu Y, Lin J, Zhao JJ, Cagnetta A, Cea M, Sellitto MA, Zhong MY, et al. Bruton tyrosine kinase inhibition is a novel therapeutic strategy targeting tumor in the bone marrow microenvironment in multiple myeloma. Blood 2012; 120:1877–87. [PubMed: 22689860]

38. Schwartz M, Zhang Y, Rosenblatt JD B cell regulation of the anti-tumor response and role in carcinogenesis. J Immunother Cancer 2016; 4:40. [PubMed: 27437104]

39. Pylayeva-Gupta Y Molecular Pathways: Interleukin-35 in Autoimmunity and Cancer. Clin Cancer Res 2016; 22:4973–8. [PubMed: 27582486]

40. Egwuagu CE, Yu CR Interleukin 35-Producing B Cells (i35-Breg): A New Mediator of Regulatory B-Cell Functions in CNS Autoimmune Diseases. Crit Rev Immunol 2015; 35:49–57. [PubMed: 25746047]

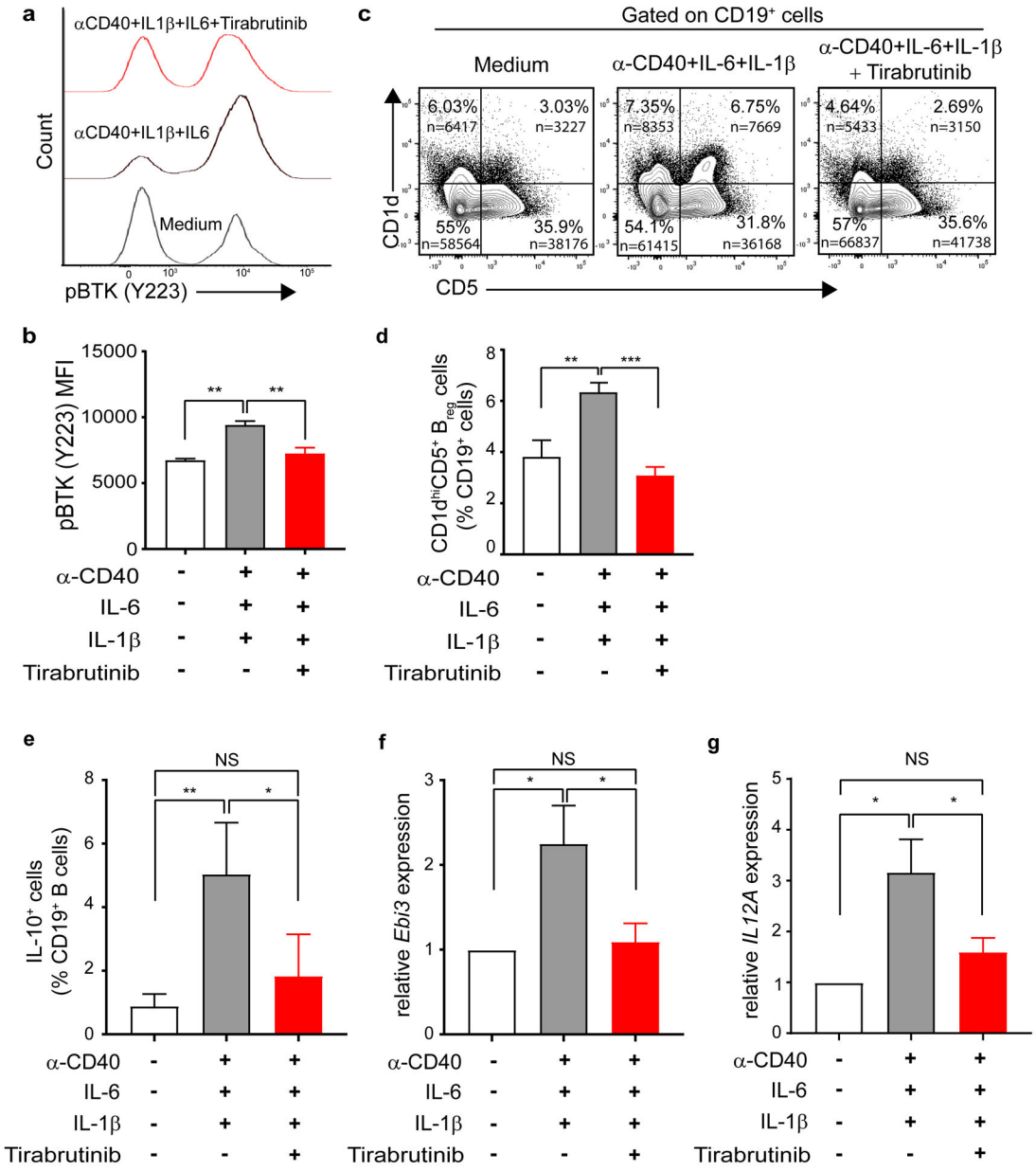

Fig. 1.

BTK activity directly regulates CD1D^{hi}CD5^{+} Breg development and function. Wild type C57BL/6 (8 weeks old, Charles River Laboratories, Wilmington, MA, USA) mice spleens were mechanically disrupted, suspended in 1%FBS/PBS, filtered through a 70-μm strainer (352350, Corning Falcon), and treated with RBC lysis buffer (00–4300-54, Thermo Fisher Scientific, Waltham, MA, USA). B cells were isolated from this single-cell suspension using CD45R (B220)-linked MACS beads (130–049-501, Miltenyi, Bergisch Gladbach, Germany) and MS columns (130–042-201, Miltenyi) as per manufacturer instructions. B cell enrichment was confirmed by flow cytometry using FITC-CD19 (6D5, 115506, Biolegend, San Diego, CA, USA) on FACScalibur (BD Biosciences, San Jose, CA, USA) and purified cells were cultured in DMEM (Gibco, Gaithesburg, MD, USA) supplemented with 10%

(v/v) FBS (Gibco) and 1% (v/v) penicillin and streptomycin (Gibco). Immediately post isolation, B cells were treated with anti-CD40 (10 ug/ml; FGK4.5/FGK45, BE0016–2, BioXCell, West Lebanon, NH, USA), IL-1β (20 ng/ml; 401-ML-005, R&D Systems, Minneapolis, MN, USA), IL-6 (20 ng/ml; 406-ML-005, R&D Systems) and tirabrutinib (5 μM, Gilead Sciences, Foster City, CA, USA) for 48 hours. **a** Representative population distribution of pBTK (Y223) expressing $CD19^+$ B cells, treated as indicated for 48h and analysed by flow cytometry on LSR II (BD Biosciences). Data were analysed using FlowJo (v10) software. Following antibodies were used as per product datasheet for flow cytometry: CD19 (6D5, #115506, Biolegend); pBTK (Y223) (N35–86, 564848, BD Biosciences). **b** Quantification of data in **a**, graph depicts median fluorescence intensity (MFI) of pBTK (Y223) staining in isolated wild type splenic $CD19^+$ B cells treated as indicated for 48 h (N=3). Error bars represent SD, *P*-value calculated using Student *t* test (two-tailed, unpaired). **, P≤0.01. Data representative of three independent experiments. **c** Representative flow cytometry analysis of isolated wild type splenic $CD19^+$ B cells treated as indicated for 48 h. Cells gated on $CD19^+$ were analysed for CD1d and CD5 expression. Following antibodies were used as per product datasheet for flow cytometry: CD19 (6D5, #115506, Biolegend), CD1d (1B1, 123509, Biolegend) and CD5 (53–7.3, 100621, Biolegend). **d** Graph depicts quantification of associated flow cytometry data in **c**, collected on LSR II (BD Biosciences) and analysed using FlowJO (v10) software, indicating $CD1d^{hi}CD5^+$ cells as percentage of $CD19^+$ B cells (N=3). Error bars represent SD; *P*-value calculated using Student *t* test (two-tailed, unpaired). **, P≤0.01; ***, P≤0.001. Data representative of three independent experiments. **e** Quantification of flow cytometric analysis of $CD19^+$ B cells treated as indicated, graph depicts $IL\text{-}10^+$ cells as percentage of $CD19^+$ B cells, N=3. Following antibodies were used as per product datasheet for flow cytometry: CD19 (6D5, #115506, Biolegend) and IL-10 (JES5–16E3, 505009, Biolegend). Error bars represent SD; P value calculated using Student *t* test (two-tailed, unpaired); *, P≤0.05; **, P≤0.01. Data representative of three independent experiments. **f, g** Graph depicting levels of *Ebi3* (**f**) and *IL12A* (**g**) mRNA expression in wild type splenic B cells, treated as indicated for 48 h and measured by qRT-PCR (N=3). RNA was isolated using an RNeasy mini kit (74104, QIAGEN, Venlo, Netherlands) and reverse transcribed using QuantiTect reverse transcription kit (205311, QIAGEN). USB HotStart-IT SYBR Green qPCR Master Mix (75762, Affymetrix, Santa Clara, CA, USA) was used for amplification. Expression was normalized to GAPDH. Fold expression was determined using the $2^{-\Delta\Delta CT}$ method. Error bars represent SD; *P*-value calculated using Student *t* test (two tailed, unpaired). *, P≤0.05. Data representative of three independent experiments. All animal care and procedures were approved by the Institutional Animal Care and Use Committee at NYU School of Medicine.

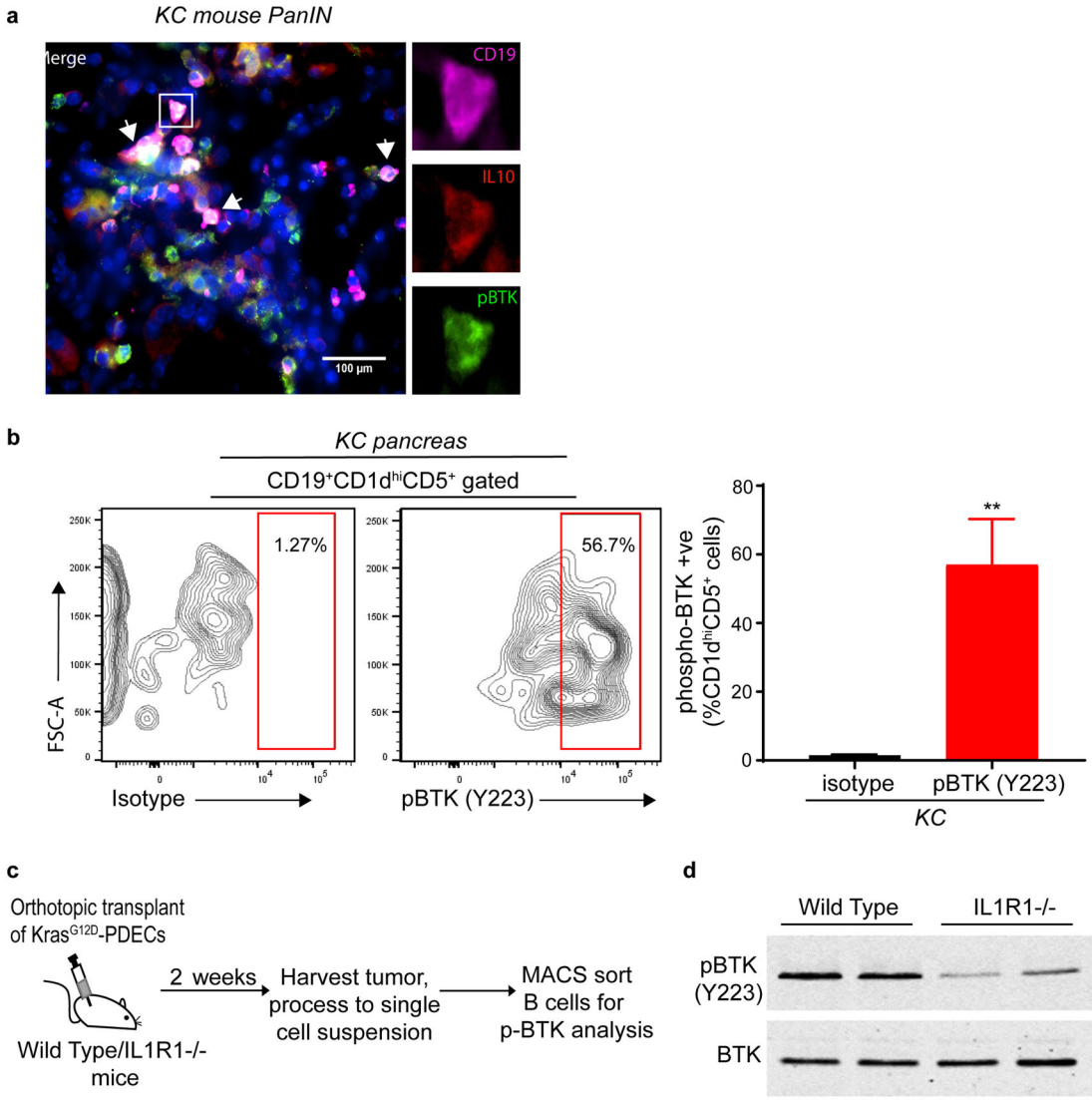

Fig. 2.

BTK is activated in PanIN-associated regulatory B cells. **a** Representative immunofluorescent staining of 2 month old *KC* mice (N=6) (31) pancreata to detect co-localisation of pBTK (Y223) with IL-10 and B cell marker CD19. Mice pancreata were fixed, processed and stained as described previously (7). Antibodies used were pBTK (Y223) (1:200, 109336, LSBio, Seattle, WA, USA), CD19 (1:50, 550284, BD Biosciences, San Jose, CA, USA) and IL-10 (1:50, sc-365858, Santa Cruz Biotechnology, Dallas, TX, USA). Slides were examined and imaged on a Nikon Eclipse Ti2 microscope. Scale bar, 100 µm. **b** Representative intracellular flow cytometric analysis of pBTK (Y223) in B cells from pancreata of *KC* mice (31), as described previously (7). Single cell suspension from pancreatic tissue was prepared as described previously (7) and stained with the following antibodies for flow cytometry analysis: CD45 (2D1, 368521, Biolegend); CD19 (6D5, #115506, Biolegend), CD1d (1B1, 123509, Biolegend), CD5 (53–7.3, 100621, Biolegend), pBTK (Y223) (N35–86, 564848, BD). After gating on the $CD45^+$ and $CD19^+$ population, cells were analysed for pBTK (Y223) expression in $CD1d^{hi}CD5^+$ B_{regs}. Also shown are

isotype controls for pBTK (Y223) staining. Graph represents quantification of FACS analysis, indicating percentage of $CD1d^{hi}CD5^{+}$ B_{reg} cells expressing pBTK (Y223) in *KC* mice (2–3 mo old, N=5). Error bars indicate SD. *P*-value calculated using Student *t* test (two tailed, unpaired). **, P≤0.01. **c** Experimental schematic for pBTK analysis of $Kras^{G12D}$-PDEC orthotopic lesions in wild type or *IL1R1−/−* mice. **d** Western blot analysis of pBTK expression in PanIN-associated wild type or *IL1R1−/−* B cells. Total B cells were isolated from 2 week old pancreatic orthotopic lesions implanted in wild type (C57BL/6J, Jackson Laboratory, Bar Harbor, ME, USA) or *IL1R1−/−* mice (B6.129S7-Il1r1tm1Imx/J, Jackson Laboratory) (N=5) using CD45R (B220)-linked MACS beads (130–049-501, Miltenyi) and MS columns (130–042-201, Miltenyi) as per manufacturer instructions. Isolated cells were lysed in sample buffer and analysed by immunoblotting on a LiCor Odyssey imager using the following antibodies: Phospho-BTK (Tyr 223) (5082S, Cell Signaling Technologies, Danvers, MA) and BTK (8547S, Cell Signaling Technologies).

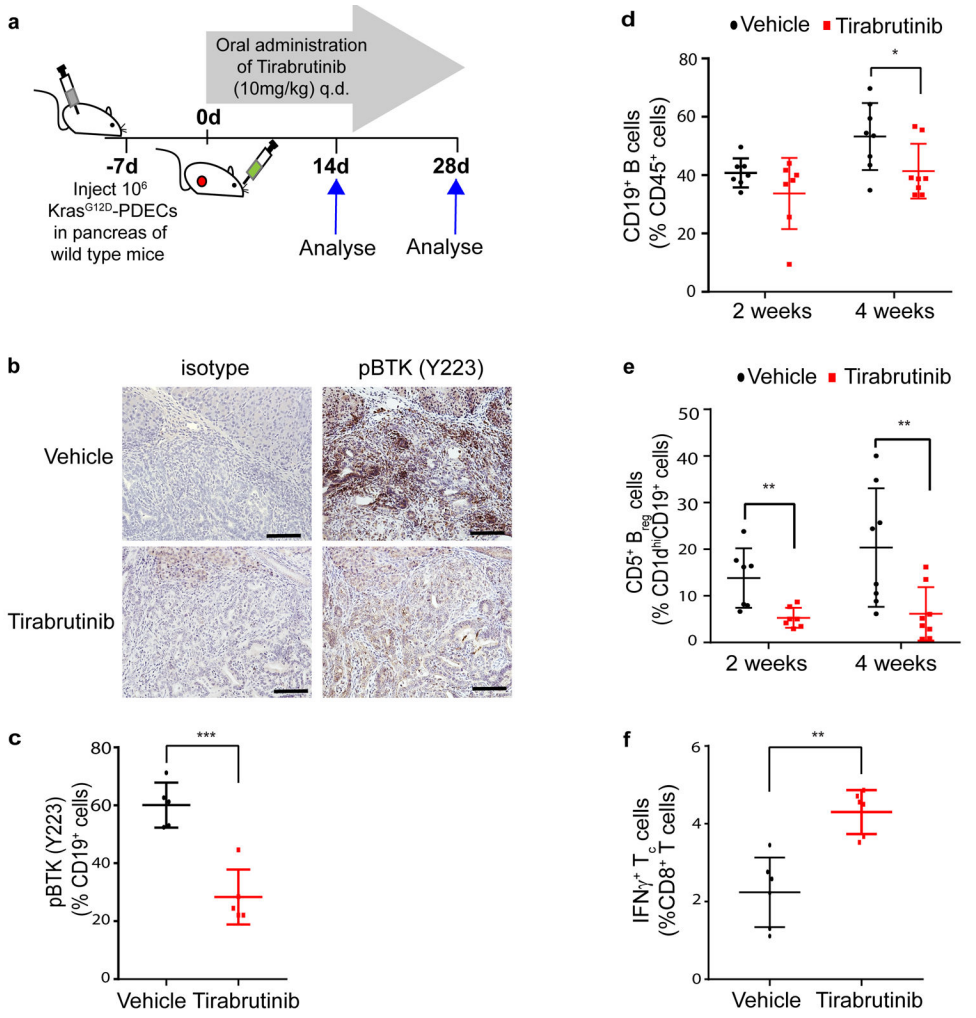

Fig 3.

BTK inhibition downregulates CD1d^{hi}CD5^{+} regulatory B cells in PanIN stroma. **a** Schema for tirabrutinib administration in PanIN-bearing mice (10mg/kg; QD; administered orally), initiated 1 week post Kras^{G12D}-PDEC orthotopic implantation. Briefly, 10^6 Kras^{G12D} PDECs were injected in the pancreas of 8 weeks old, female C57BL/6 mice (Charles River). PanIN-bearing mice were randomly assigned to control and experimental groups for subsequent drug treatment Sample sizes for experiments were determined without formal power calculation. Investigators were not blinded to group allocation or outcome assessment. **b** Representative immunohistochemical detection of stromal pBTK (Y223) in Kras^{G12D}-PDEC orthotopic lesions treated with vehicle or tirabrutinib for 2 weeks. Mice pancreata were fixed, processed and stained by immunohistochemistry (IHC) as decribed previously (7). Antibodies used were pBTK (Y223) (1:200, 109336, LSBio, Seattle, WA, USA). Slides were examined and imaged on a Nikon Eclipse 80i microscope. Scale bar, 200 μm. **c** Quantification of intracellular flow cytometric analysis of pBTK (Y223) expression in CD19^{+} B cells from Kras^{G12D}-PDEC orthotopic lesions treated with vehicle or tirabrutinib for 2 weeks (N=7). Error bars indicate SD; *P*-values determined by the Student *t* test (two-tailed, unpaired); ***, P<0.001. **d** Quantification of flow cytometric analysis of CD19^{+} B

cells from vehicle or tirabrutinib treated $Kras^{G12D}$-PDEC orthotopic lesions for 2 and 4 weeks. (N=7, 2 weeks treatment cohort; N=8, 4 weeks treatment cohort). Error bars indicate SD; *P*-values determined by the Student *t* test (two-tailed, unpaired). *, P≤0.05. Data representative of two independent experiments. **e** Quantification of flow cytometric analysis of $CD1d^{hi}CD5^{+}$ Breg cells from vehicle or tirabrutinib treated $Kras^{G12D}$-PDEC orthotopic lesions for 2 and 4 weeks. Cells gated on $CD19^{+}CD1d^{hi}$ were analysed for CD5 expression, graph represents $CD5^{+}$ cells as percentage of $CD19^{+}CD1d^{hi}$ B cells. (N=7, 2 weeks treatment cohort; N=8, 4 weeks treatment cohort). Error bars indicate SD; *P*-values determined by the Student *t* test (two-tailed, unpaired). **, P≤0.01. Data representative of two independent experiments. **f** Quantification of intracellular flow cytometric analysis of IFNγ expression in $CD8^{+}$ T cells isolated from $Kras^{G12D}$-PDEC orthotopic lesions treated with vehicle or tirabrutinib for 2 weeks (N=6). Cells gated on $CD45^{+}CD3^{+}CD8^{+}$ were analysed for IFNγ expression. Following antibodies were used as per product datasheet for flow cytometry: CD45 (2D1, 368521, Biolegend); CD3 (145–2C11, 100327, Biolegend); CD8 (53–6.7, 100713, Biolegend), IFNγ (XMG1.2, 11–7311-82, Thermo Fisher Scientific). Error bars indicate SD; *P*-values determined by the Student *t* test (two-tailed, unpaired). **, P≤0.01.

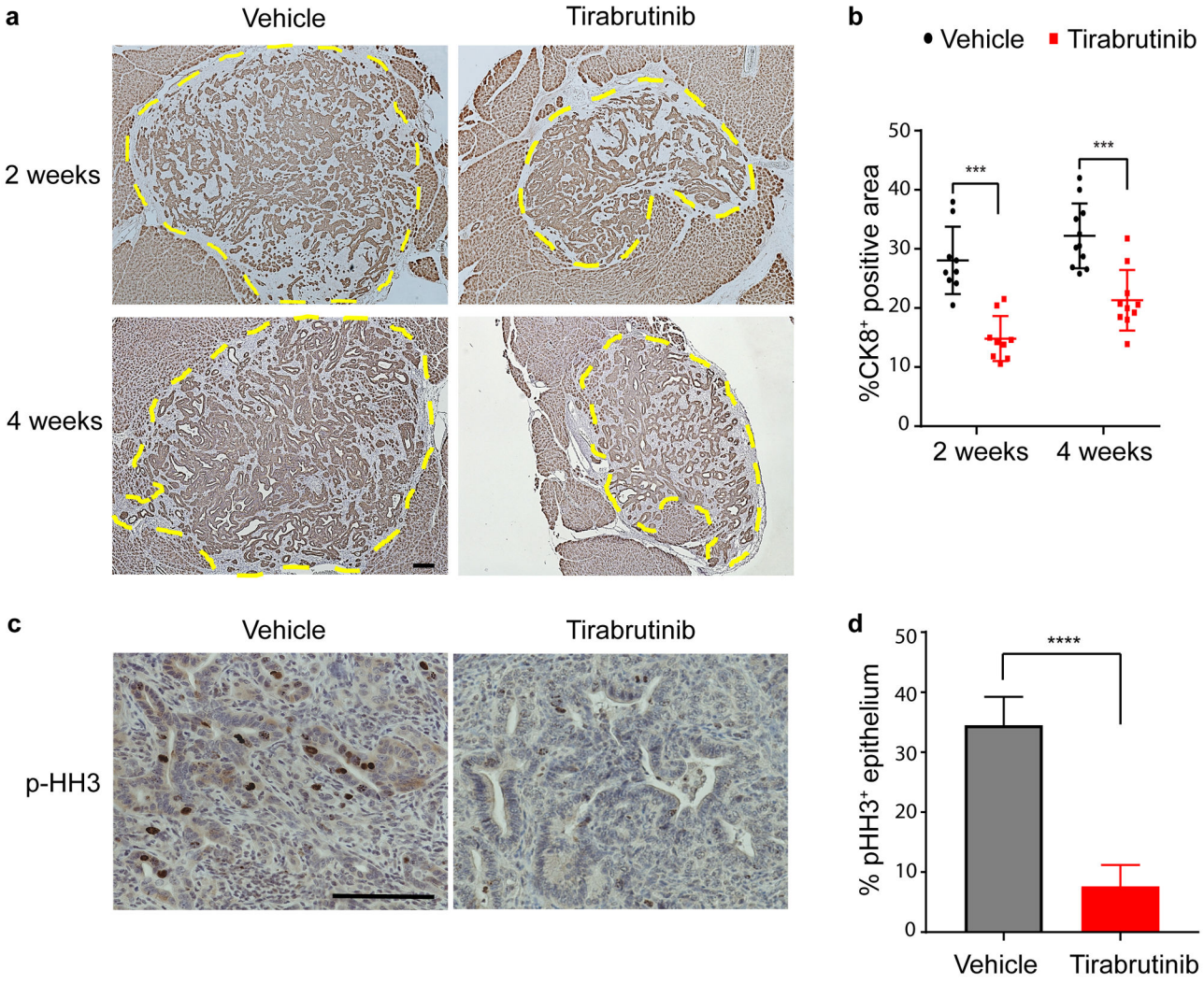

Fig. 4.

Tirabrutinib treatment inhibits proliferation and restricts growth of $Kras^{G12D}$-PanIN lesions. **a** Immunohistochemical detection of CK8 in sections of $Kras^{G12D}$-PDEC orthotopic lesions treated with tirabrutinib or vehicle control for 2 and 4 weeks as indicated. Representative images are shown. Mice pancreata were fixed, processed and stained by immunohistochemistry (IHC) as decribed previously (7). Antibody used was CK8 (1:200, TROMA-Ic, DSHB, University of Iowa; Iowa City, IA, USA). Slides were examined and imaged on a Nikon Eclipse 80i microscope. Scale bar, 200 μm. **b** graph depicts quantification of data from **a** indicating % $CK8^+$ area within the lesion, determined using ImageJ software. (N=9, Vehicle, 2 weeks; N=9, tirabrutinib treament, 2 weeks; N=11, Vehicle, 4 weeks; N=10, tirabrutinib treatment, 4 weeks). Error bars indicate SD; *P*-value calculated using Student *t* test (two-tailed, unpaired). Data representative of two independent experiments. ***, P≤0.001, **c** IHC staining for phospho-Histone H3 (p-HH3) of $Kras^{G12D}$-PDEC orthotopic lesions treated with tirabrutinib or vehicle control for 2 weeks. Representative images are shown. Antibody used was phospho-Histone H3 (1:200, 06–570, Millipore). Scale bars, 200 μm. **d** graph depicts quantification of data in **c** indicating percent

positive p-HH3 staining in epithelial cells using ImageJ software (10 fields of view per animal; N=7). Error bars indicate SD; *P*-values determined by the Student *t* test (two-tailed, unpaired); ****, P≤0.0001. Data representative of two independent experiments.